

Robotic magnetic steering and locomotion of capsule endoscope for diagnostic and surgical endoluminal procedures

Gastone Ciuti†, Pietro Valdastri†,* , Arianna Menciassi†,‡
and Paolo Dario†,‡

† *Scuola Superiore Sant'Anna – CRIM Lab, Pisa, Italy*

‡ *IIT, Italian Institute of Technology Network, Genova, Italy*

(Received in Final Form: July 23, 2008. First published online: October 26, 2009)

SUMMARY

This paper describes a novel approach to capsular endoscopy that takes advantage of active magnetic locomotion in the gastrointestinal tract guided by an anthropomorphic robotic arm. Simulations were performed to select the design parameters allowing an effective and reliable magnetic link between the robot end-effector (endowed with a permanent magnet) and the capsular device (endowed with small permanent magnets). In order to actively monitor the robotic endoluminal system and to efficiently perform diagnostic and surgical medical procedures, a feedback control based on inertial sensing was also implemented. The proposed platform demonstrated to be a reliable solution to move and steer a capsular device in a slightly insufflated gastrointestinal lumen.

KEYWORDS: Robotic platform; Locomotion and steering by magnetic forces; Endoluminal surgery; Capsular endoscopy.

1. Introduction

Traditional techniques for endoluminal procedures in the gastro intestinal (GI) tract adopt flexible endoscopes, which are introduced into the oral or rectal orifices. Such techniques enable a reliable diagnosis and are currently a viable solution to manage many diseases of the digestive district. Advanced endoscopic technologies are extensively reviewed in Reavis *et al.*,¹ showing enhanced capabilities in both diagnosis and therapeutic procedures towards the new frontier of natural orifices transluminal endoscopic surgery (NOTES).² Flexible endoscopes usually have a steerable tip in order to orient the diagnostic or the therapeutic unit towards the place of interest. The ability to steer the distal part is generally obtained by cable actuation, with the control knob placed on the external part of the endoscopic device. The cables providing mechanical actuation run through the whole length of the instrument, making it quite rigid and with a large diameter (typically 13 mm for a standard colonoscope). This results in a limited accessibility and makes gastroscopic and colonoscopic procedures considerably traumatic and frequently poorly tolerated by patients.³ A significant

advancement in terms of accessibility occurred mainly in the diagnostic field with the advent of wireless capsular endoscopy (WCE).⁴ This approach enables a non-invasive diagnosis of the GI tract with high potential for screening. Commercial devices exploit peristalsis to move passively along the GI tract.⁵ Therefore they are forced to go ahead without the possibility of stopping, turning or going back during their journey. This explains why the majority of clinical failures of WCE are related to an incomplete small-bowel examination.⁶ This represents one of the main limits of these devices. Capsules endowed with active locomotion would allow a direct remote control on the steering and orientation of the device toward suspicious spots. This would also enable therapeutic procedures, such as surgical clip releasing and localized drug delivery, to be performed by wireless capsule robots.⁷

There are mainly two strategies for providing a swallowable capsule with active locomotion.⁸ One is pursuing the miniaturization of locomotion systems to be integrated onboard the capsule.^{9–11} The main limit of this approach is the high amount of energy to be stored on board in order to actuate the mechanism. Furthermore, the limited volume available for both the locomotion mechanism and the energy source makes the system integration quite challenging. The Given Imaging PillCam¹² is 11 mm in diameter and 26 mm long and it embeds a vision unit, a telemetric link and a battery pack, but it does not possess locomotion mechanisms: the addition of a locomotion unit and an extra energy tank would make the final device hard to swallow.

The other alternative relies on an external approach where actuation, generally based on magnetic fields, is outside the capsule. This reduces the required capsule payload to small magnets or coils, and relieves the power budget of the wireless device. In Carpi *et al.*¹³ a couple of stacked permanent magnets is handheld by the operator to steer an endoscopic capsule. Although this approach is cheap and flexible, low precision of movements, due to hand control, impairs outcomes of diagnostic and surgical procedures. A similar approach is currently under investigation by Given Imaging Ltd. in the framework of the European Project 'NEMO'.¹⁴

A possible solution to enhance steering performances is to generate the electromagnetic field by electromagnets with

* Corresponding author. E-mail: pietro@sssup.it

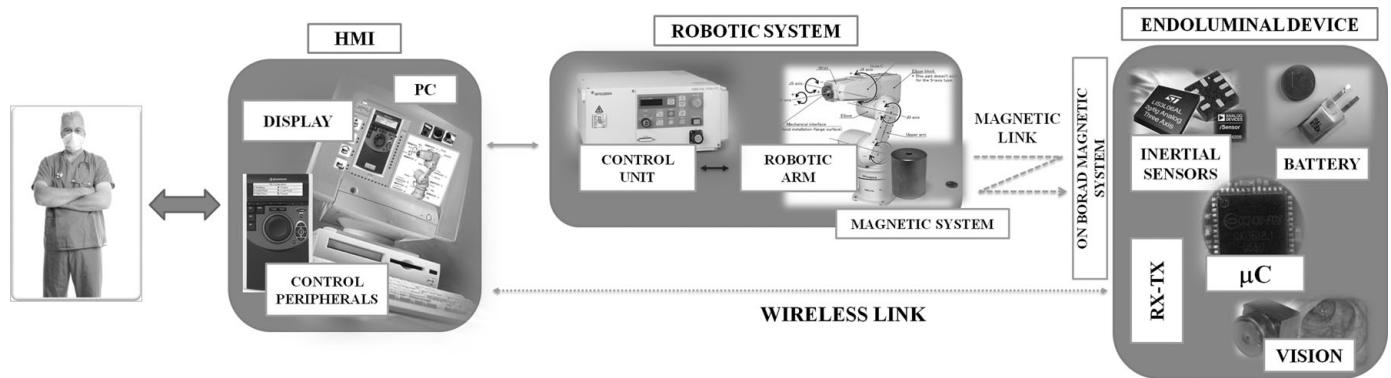


Fig. 1. System architecture of the proposed robotic platform.

automated operation.^{15,16} This approach may lead to very high position accuracy down to the micro- and nanoscale, as in the works proposed by Abbot *et al.*¹⁷ or Tamaz *et al.*¹⁸ However, its main limitation is that bulky equipment, with at least three orthogonal coils, is usually required to generate a variable and controllable field.

An interesting solution is proposed by Stereotaxis¹⁹ (Stereotaxis, Inc, St. Louis, USA) for catheter tip orientation. The system takes advantage of two permanent magnets mounted on articulated or pivoting robotic arms that are enclosed within a stationary housing, with one magnet on either side of the patient table. This external unit works in synergy with a catheter embedding a small permanent magnet in its tip. Thanks to the symmetrical placement of the external magnets, the magnetic field may be cancelled in precise locations of the operative scenario. Further, a small misalignment of the two magnets, obtained by precise robotic steering, can induce a localized magnetic field, thus enabling fine orientation of the catheter tip. This system, even if it is not able to generate high forces on the distal device, is an interesting example about how robotics may improve therapeutic procedures thanks to high precision and predictability of movements.

An approach based on robotic manipulation of an external permanent magnet for a precise locomotion and orientation of a swallowable robotic pill is described in this paper. A complete platform for an effective translation, rotation and roto-translation of a magnetic capsule robot for diagnostic and surgical procedures will be described in details. This paper is organized as follows: Section 2 describes the magnetic locomotion platform, emphasizing the robotic system in Section 2.1, the magnetic link in Section 2.2 and the sensorial feedback in Section 2.3. Section 3 reports the results obtained during *ex-vivo* experiments. Finally, conclusions are reported in Section 4.

2. Magnetic Locomotion Platform

The proposed system, schematically represented in Fig. 1, is composed by a human machine interface (HMI), a 6 degrees of freedom (DOF) robotic arm able to move an external permanent magnet (EPM) and a capsular device, provided with inertial and vision wireless sensors and a

set of permanent magnets (internal permanent magnets, IPM).

The HMI displays the real time images coming wirelessly from the capsular device together with several information related to the state of the platform. The medical doctor can interact with the system through an intuitive input device, imposing motion to the robotic arm by a dedicated control loop. Thanks to the interaction between the EPM, mounted as end-effector of the robotic arm, and several IPM inside the capsular device, the motion imposed by the user is transmitted to the wireless unit.

In the present work, the capsular device embeds just the sensorial functions related to an effective visual control and a closed loop magnetic steering. Additional features, related to the peculiar surgical or diagnostic application, can be included on board. Thanks to the limited volume required for magnetic steering, compared to internal locomotion solutions (e.g. approximately 2374 mm³ in the legged device presented by Quirini *et al.*¹¹), additional space may be available for other functions.

The first issue addressed in the system design was the setup of the robotic arm control through an intuitive HMI, thus allowing a real time and precise movement of the end-effector by the medical doctor. Then, a proper dimensioning of the magnetic link was addressed, in order to achieve an effective magnetic interaction between the EPM and the IPM. Finally we developed an innovative sensing strategy, based on inertial and visual information, to close the control loop with the robotic arm and to enhance the feedback to the user. In the following subsections, the above issues will be explained in details.

2.1. Robotic system

One of the first issues to be considered in order to design a practical medical robotic platform is the console, which interfaces with the staff that is going to perform the procedure. Acceptability and usability must be addressed at the very beginning by a proper design of the HMI. For this reason, we developed a user-friendly interface that bridges the robotic arm with the user by a dual video system and a multi DOF controller. A schematic design of this architecture is represented in Fig. 2.

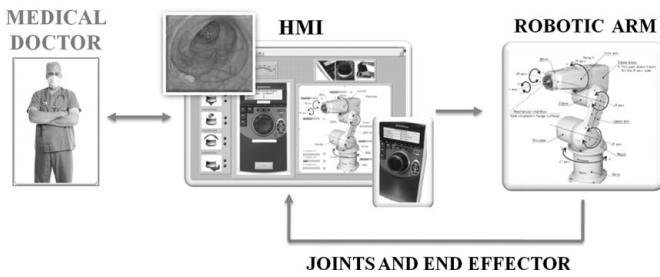


Fig. 2. Master side: control loop of the robotic platform.

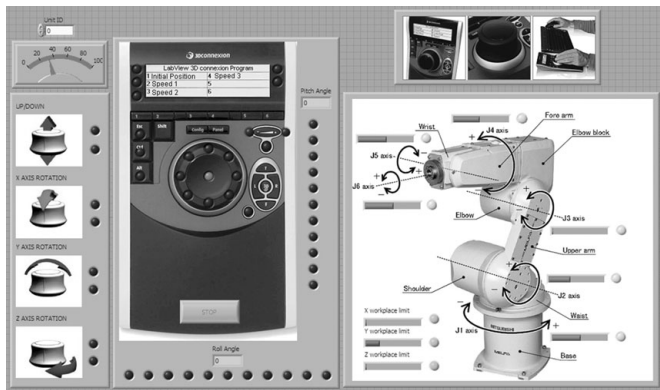


Fig. 3. Virtual control panel of the developed HMI.

A real time image stream coming from a wireless camera located in the endoluminal device can be displayed on a first video screen. This already enables an effective diagnosis by the medical doctor. A second video unit shows a virtual control panel as in Fig. 3.

The control panel, developed with LabVIEW (National Instruments, Inc., USA), was designed to display the status and several relevant control information of the robotic platform. In particular it presents to the user the speed and direction of the end-effector, the distance from the workspace limits for each DOF, the wireless signal strength, the battery level of the capsular device and the information regarding pitch and roll. These are all the information we considered relevant for a correct and effective operation of the developed system.

An additional feature is the possibility to define a custom workspace for the end-effector, in order to adapt the robotic arm movements to the specific patient undergoing the procedure. This customization process is a simple numerical adjustment of both the workspace centre in a tri-dimensional space and the maximum allowed travelling range for each DOF. Further developments may include a workspace trimming by importing a preoperational tomography of the patient's abdomen.

Another important component of the HMI is the 6 DOF control device (3D SpacePilot, 3D connexion Inc. USA). This is a user-friendly interface, perfectly suitable for a direct control of the end-effector. It allows the execution of translational and rotational movements through a single knob. A view of this input device is reported also on the

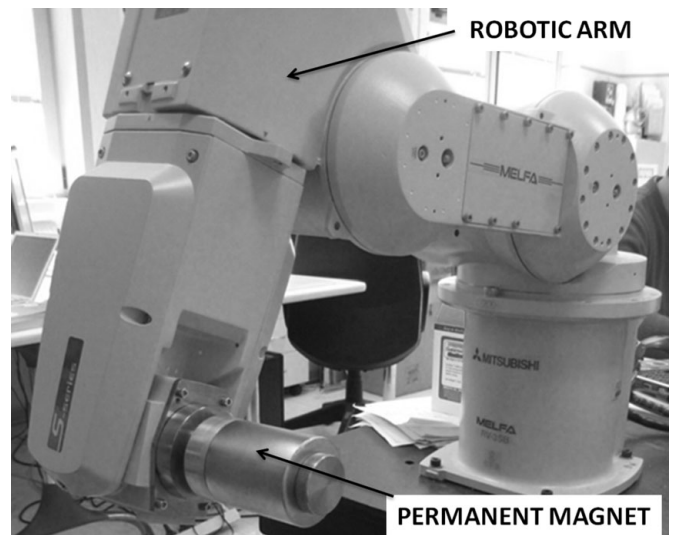


Fig. 4. The anthropomorphic robotic arm with the EPM mounted as end-effector.

virtual control panel, as represented in Fig. 3, where several visual indicators are used to display its actual status.

Programmable buttons, located on the controller, enable macro operations to be performed. In particular, three different end-effector speed levels can be directly selected, e.g. 2.5 mm/s, 5 mm/s and 10 mm/s.

As regards the anthropomorphic robotic arm, a 6 DOF industrial robot RV-3SB, produced by Mitsubishi Electric. (Fig. 4), was used.

The robotic arm is equipped with absolute encoders in every joints. The workspace of the robot is approximately a portion of a sphere and the farthest point that can be reached by the end-effector is 64.2 cm away from its base. Movement resolution is ± 0.02 mm, ensuring an accurate positioning of the end-effector.

A low level control of the robotic arm is implemented by using Cosirop 2.0, a Mitsubishi Electric programming platform, that allows simple functions to be written in a Basic-like language (Melfa Basic IV) and uploaded to the robotic controller by TCP/IP communication.

A high level, real-time control architecture of the robotic arm has been implemented by following the architecture of Fig. 5.

The HMI, running on a personal computer (PC), establishes a bidirectional communication with the robotic arm, controlling the end-effector as imposed by the user on the input device. The chosen direction of movement is decoded by the HMI, which calls the proper low-level subroutine, thus producing the corresponding incremental movement of the robotic arm. At the end of every movement, the angle of each joint and the end-effector configuration, in terms of position and orientation, are acquired and immediately sent to the HMI to be displayed on screen. Particular emphasis was devoted to minimize the transmission time in order to obtain a real time control and a bidirectional communication flow. The refresh rate of the control loop is 225.2 ms, thus enabling a smooth and real-time motion of the end-effector.

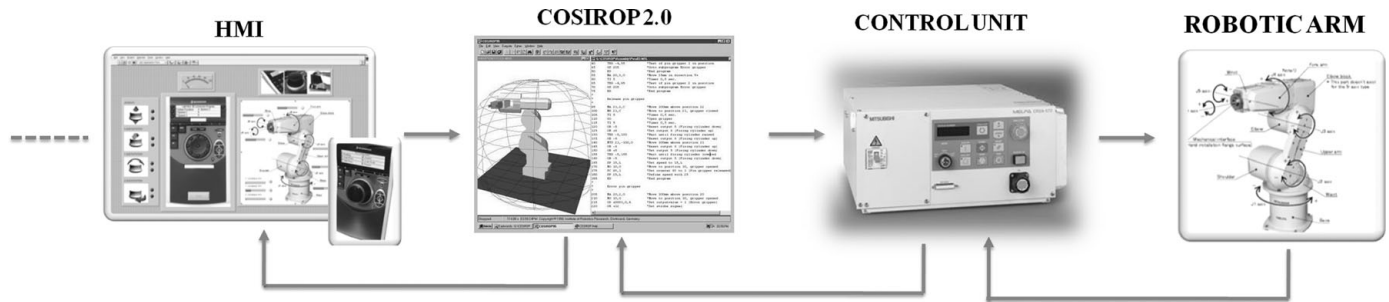


Fig. 5. Communication flow between the user and the robotic arm.

Having a fast and reliable communication would also allow to prevent the end-effector to exceed the imposed workspace.

a precise magnetic steering can be used to orient the device towards the target.

2.2. Magnetic system

In order to perform endoluminal procedures with the proposed platform, an effective and reliable magnetic link must be established between the end-effector and the wireless device. Specifically, our main target is to maximize the magnetic interaction forces and torques induced by an EPM on the endoscopic capsule having multiple IPM on board, still complying with the limitations imposed by the specific applicative scenario. Furthermore, we aim to obtain gentle and precise pitch and yaw capsule steering by simple movements of the EPM.

A complete analytical solution for the forces between two permanent magnets is reported in J. S. Agashe *et al.*²⁰ This is based on the Kelvin's formula and the Biot-Savart's law. Considering those physical relations and our specific goals, the following design parameters should be defined:

- (i) *Size of EPM.* A trade-off between magnetic attraction force and payload constraints of the robotic arm must be considered.
- (ii) *Magnetic properties of EPM.* Magnetic flux density should be maximized by proper material selection. The magnetization direction may also be properly selected in order to obtain particular features for the magnetic link.
- (iii) *Size of IPM.* Since the size of the wireless endoluminal device should be minimized, a trade-off between the magnetic attraction force and the capsule payload must be defined.
- (iv) *Magnetic properties of IPM.* Also in this case, the maximization of magnetic flux density should be considered for material selection of the IPM. In addition, the magnetization direction should be selected accordingly to the one of the EPM in order to achieve the desired features for the magnetic link.
- (v) *Arrangement of IPM inside the capsule.* An optimal arrangement of the IPM may improve the magnetic link quality. Furthermore, a proper placement of the IPM would enable the wireless device to better engage the lumen walls in a pre-defined position, since it will align in an intermediate position according to the superimposed field lines of the IPM. This feature would be beneficial in the case of surgical procedures, where

To identify the above defined parameters, a reference benchmark in terms of system performance was required to guide the magnetic link design phase. A quantifiable goal for the platform may be to lift a capsular device in a slightly insufflated lumen, with the end-effector of the robot placed at a safe distance from the patient's body.

The capsule robot would have the basic functions as the Given Imaging PillCam, i.e. vision, illumination, power supply and telemetry. In addition, it will be provided with IPM and would integrate specific surgical or diagnostic sub-modules. A rough but conservative weight prediction for such a device may be ten times the PillCam (3.22 g), considered a golden standard for capsular endoscopy. As regards the EPM-IPM typically working distance, we assume 150 mm. Considering all these issues, the magnetic link we are targeting should be able to lift a device having a weight of 32 g with the end-effector placed 150 mm away from the capsule. This results in an attraction force of about 315 mN that the EPM must exert on the wireless device.

In order to optimize design parameters 1 and 2, a NdFeB N35 permanent magnet (Sintered NdFeB-magnets, B&W Technology & Trade GmbH, China), having a cylindrical shape, was selected as EPM. It has a diameter of 60 mm, a length of 70 mm and a weight of 1.5 kg. In addition, it has a coaxial hole that was used to fix the EPM to the robotic arm. Given the payload allowed by the robotic arm, this choice maximizes the volume of the EPM that can be safely supported. The EPM is magnetized perpendicularly to the main axis²¹ with a magnetic flux density of 1.21 T. The magnetization direction and the cylindrical shape were purposely selected among other possible solutions to finely impose pitch and yaw on a second device having permanent magnets oriented along its main axis. According to this, we selected the IPM shape and magnetization direction to be respectively cylindrical and parallel to the main axis of the capsule. To finalize the design parameter 4, NdFeB was chosen also for the IPM for its high magnetic field strength.

To avoid possible interferences by the EPM on the robotic arm electronic circuitry a cylindrical aluminium profile, with diameter of 60 mm and thickness of 20 mm, was placed between the end-effector and the EPM. This acts as a spacer, thus reducing the magnetic flux density inside the robotic arm structure. Aluminium has been selected for its light weight.

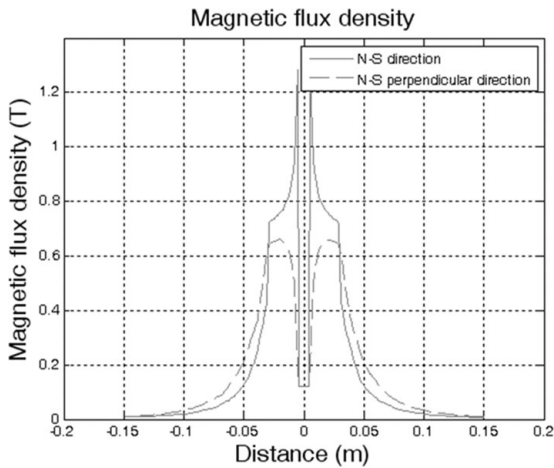


Fig. 6. EPM magnetic flux density plot.

Once parameters 1, 2 and 4 were defined, a simulation framework was developed by using COMSOL Multiphysics 3.4 (COMSOL Inc., Sweden) in order to properly fix the design parameters 3 and 5.

An initial registration phase was performed by comparing simple simulation results with real force data from the interaction between the EPM and a NdFeB N35 reference permanent magnet, having a diameter of 3 mm, a length of 10 mm and a residual magnetic flux density equal to 1.21 T. The force data were acquired with a high precision load cell (FMI-210, Alluris, Germany). This allowed to find a proper trade-off between computational burden and simulation accuracy. The selected mesh consisted of about 450,000 elements, with a maximum element size fixed to 1/50 of the maximum geometric feature in the scenario. The incremental ratio of the mesh elements was fixed to 1.3. The mesh curvature factor and the mesh curvature cut-off were chosen equal to 0.2 and 0.001 respectively.

Thanks to simulations, we obtained the distribution of magnetic flux density of the EPM from the centre up to a radial distance of 200 mm in the N-S magnetic direction and in the perpendicular direction (Fig. 6). From those plots it is possible to observe how the magnetic flux density falls quickly with the distance, reaching a negligible value 200 mm away from the EPM centre.

The simulation platform was then used to select the best size and arrangement for the IPM. A typical simulation screenshot is represented in Fig. 7.

The space between the EPM and the capsular device was considered filled with water, in order to simulate the presence of surrounding abdominal tissues from a magnetic susceptibility viewpoint. This is in the range of 10^{-6} for both water and biological tissues.²²

For each configuration of parameters, attraction and translation forces, together with induced torques, were simulated at a distance from the EPM ranging between 50 mm to 200 mm. In particular, in order to evaluate translation force, the EPM was moved 50 mm along the axis parallel to the translational movement of the device, while for calculating the magnetic torque the EPM was rotated 30° around the axis going from the EPM to the endoluminal capsule.

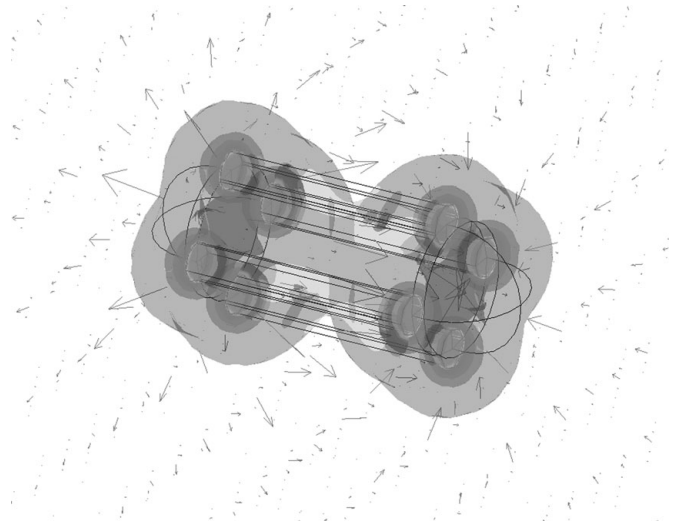


Fig. 7. Simulation screenshot of IPM arranged symmetrically on the capsule surface. In this case we used 4 permanent magnets having a diameter of 3 mm, a length of 20 mm and a residual magnetic flux density of 1.21 T.

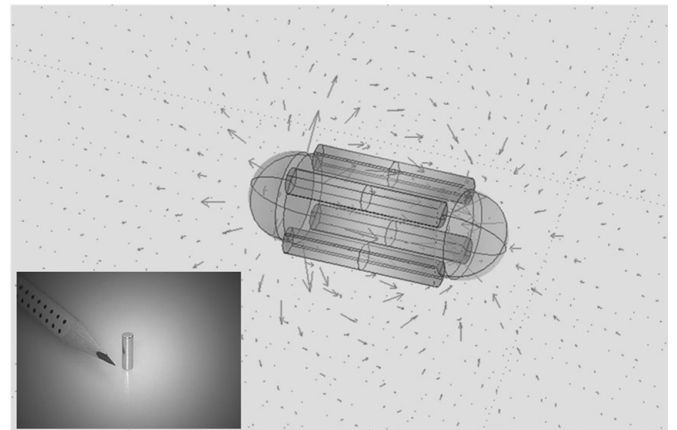


Fig. 8. Simulation screenshot of the selected IPM configuration – the single IPM is represented on the left.

Simulations were performed to find out the minimum volume for the IPM, once given the material, shape and the magnetization direction, that would allow to meet the specified goal in terms of attraction force (315 mN). A single magnet with the aforementioned specifications, but with a variable volume, located in the centre of the capsule, was considered as IPM. A standard commercial cylindrical magnet (MTG Europe Magnet Technology Group, Germany) having a diameter of 3 mm, a length of 10 mm, axial magnetization and magnetic flux density of 1.21 T, was selected as size unit (about 70 mm^3). This is represented in the lower left corner of Fig. 8. We varied the volume of the IPM from 420 mm^3 (6 units) to 630 mm^3 (9 units) in 4 equivalent steps. The minimum volume required to achieve an attractive force in the range of the targeted one is 560 mm^3 , corresponding to 8 units.

Once the parameter 3 and 4 were fixed, we run a second set of simulations where the selected volume of magnetic material was arranged in four different positions:

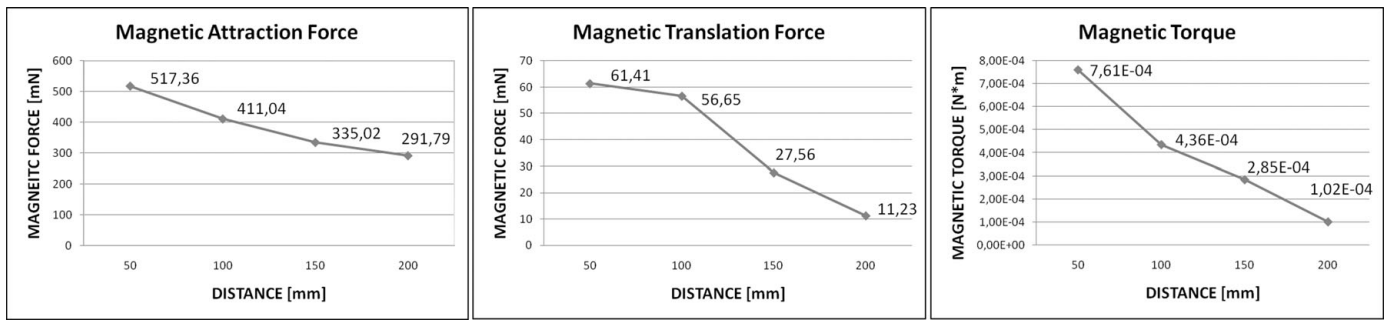


Fig. 9. Magnetic attraction force, magnetic translation force and magnetic torque for the selected EPM-IPM configuration at several distances for the configuration D (in the second plot the EPM is moved 50 mm along the axis parallel to the translational movement of the device, while for the third plot the EPM was rotated 30° around the axis going from the EPM to the capsule).

- A single cylinder having a volume of 560 mm³ located in the centre of the capsule,
- Two cylinders, 280 mm³ each, placed symmetrically on two sides of the capsule,
- Three cylinders, 186 mm³ each, arranged on the external surface of the capsule at 120° each other,
- Four cylinders, 140 mm³ each, arranged on the external surface of the capsule at 90° each other.

In configurations B to D, the axes of the cylindrical magnets lie on the capsule external circumference.

Configuration D resulted the best in maximizing both the magnetic forces and the radius of the solid cylinder of space available inside the capsule. This last feature is highly desirable from a system integration standpoint.

Configuration D, represented in Fig. 8, was achieved by placing four couples of the cylindrical magnets mentioned above as size unit (MTG Europe Magnet Technology Group, Germany).

The simulated forces resulting with the described parameters selection for both EPM and IPM are plotted against the distance between the EPM and the capsular device (Fig. 9).

In particular, the magnetic attraction plot shows that the selected parameters enable the platform to meet, and even overcome, the goal we are targeting (315 mN), since the attraction force 150 mm away from the EPM is 335 mN. The effectiveness of the defined benchmark for the design of the magnetic link parameters will be discussed in Section 3, where experimental tests are reported. In particular, the designed magnetic link should demonstrate strong enough to reliably drag and steer the capsular device.

2.3. Sensorial feedback

At high level, the control loop of the robotic platform is closed by the user, who maneuvers the capsule depending on the images delivered by the on board camera. Therefore, the endoluminal device has been provided with a wireless vision module. This is composed by a CMOS camera (MO-S508W-A001, Misumi Manufacturer & Exporter, Taiwan) and four white light emitting diodes (LED). The image stream is transmitted to the HMI and displayed on a dedicated video screen.

However, vision feedback is not enough for a complete control of the device. A localization system would enable

the medical doctor to know the exact position and orientation of the capsule. A magnetic localization system, such as the Aurora NDI,²³ would be the ideal candidate to accomplish this function. However, the permanent magnet used here for locomotion and steering would disturb the electromagnetic field, thus preventing a reliable localization. For this reason a different approach, based on inertial sensing, has been pursued in order to solve mainly two problems. The first is to understand where the device is located inside the patient body, so that the robotic arm can stop the end-effector in a precise operative position. At this point, the IPM may not be aligned to the magnetic field generated by the EPM. This condition would prevent the capsular device to move as desired by the user. Therefore, a procedure must be conceived to align the EPM field to the IPM streamlines, so that a pitch movement of the EPM translates in a corresponding adjustment of the IPM.

To address those issues, a digital tri-axial accelerometer (LIS331DL, STMicroelectronics, Switzerland) was integrated in the capsule. This sensor was connected to a microcontroller (CC2430, Texas Instruments, USA) by a serial peripheral interface (SPI) communication port. The microcontroller, thanks to an embedded IEEE 802.15.4 compliant transceiver, was used to send the data gathered from the accelerometer to the HMI. This electronic subsystem was developed on a round shape double layer board having a diameter of 9.6 mm and a thickness of 3 mm. Thanks to its small dimensions, the acceleration sensing unit can be embedded in a pill size device in order to enable inertial feedback as described in the following paragraphs. The sensor resolution is 0.35 m/s² and the sampling time is 50 ms. The HMI receives the information by a purposely developed wireless interface connected to a dedicated universal serial bus (USB) port of the PC.

As soon as the medical procedure begins and the wireless device is inserted in the patient body, the robotic platform can start the localization procedure. This consists of a pre-programmed scanning performed by the robotic arm. When the end-effector, carrying the EPM, gets close to the endoluminal device, the wireless capsule is attracted towards the EPM, stopping its motion at the lumen wall, as represented in Fig. 10.

This translates in an acceleration spike mainly on the vertical component, as reported in Fig. 11.

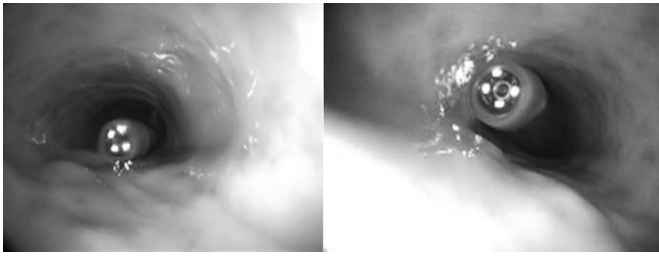


Fig. 10. Magnetic attraction of the capsule on the internal surface of the GI tract during the localization procedure.

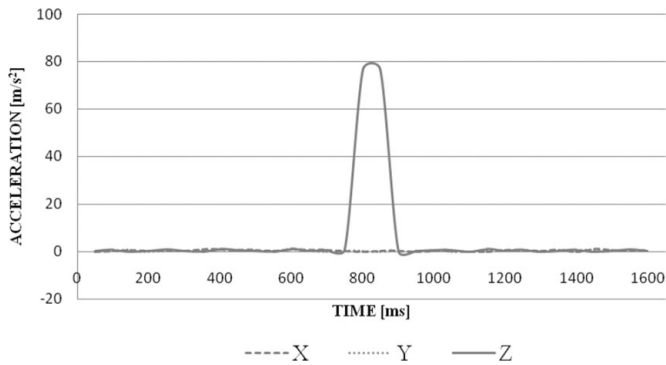


Fig. 11. Typical acceleration plots when the EPM approaches the IPM during the localization procedure.

This event can be tracked by the inertial sensor and fed back to the HMI, which gets the information about the wireless device location.

In the case this procedure fails to identify the capsule position, it is automatically repeated reducing the distance between the EPM and the patient’s abdomen. The spatial resolution of this localization method is mainly related to the environment where the capsule is located. If the capsule is constrained in a certain position by a considerable amount of surrounding tissue, then the localization resolution will be pretty high, because the capsule will be attracted only when the EPM is above it. Otherwise, in the case the capsule is located in a loose organ, it will be attracted by the magnet earlier in the scanning procedure, thus resulting in a lower spatial resolution. Anyway, in both those conditions, we are able to effectively localize the capsule and to establish a reliable magnetic link between the EPM and the IPM as will be further detailed in Section 3.

Once an effective position for magnetic steering has been reached by the end-effector, the magnetic field orientation of the EPM and the IPM must be aligned, as previously explained. This kind of registration can be performed by rotating the end-effector and monitoring the accelerometer output. In this case the inertial sensor would be used as an inclinometer and the pitch (i.e. the rotation of the capsular device around the *b*-axis reported in Fig. 12) would be sampled.

This task is completed as soon as the inclination signals starts following the rotation of the EPM.

Pitch and roll are useful also for the rest of the surgical or diagnostic procedure, since they provide information about the magnetic link quality. This can be considered acceptable if an angular movement of the EPM translates

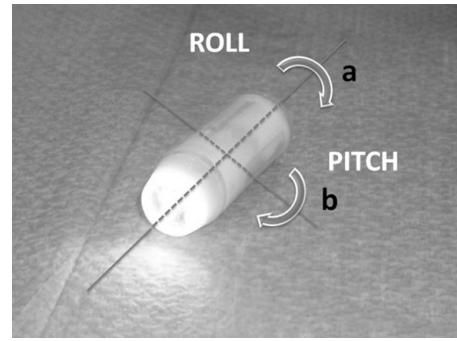


Fig. 12. Roll (a) and pitch (b) for the capsular device.

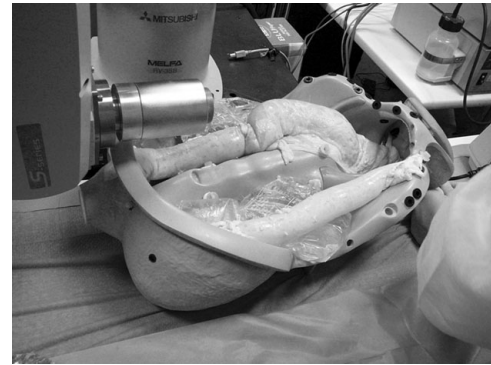


Fig. 13. The LGI phantom model.

in a corresponding inclination of the capsular device. For this reason, the signals coming from the inertial sensors are continuously sampled and displayed on the HMI with a resolution of 6°.

3. Experimental Results

Extensive bench tests were performed to evaluate the performance of the overall robotic platform in *ex-vivo* conditions. These tests were carried out in a lower-GI tract (LGI) phantom model as illustrated in Fig. 13. It consists of an anatomical model of the abdominal chest and pelvic cavities, with additional accessories to simulate organs (e.g. spleen, liver and sphincter). This phantom has fixtures aligned in the shape of human mesentery for the attachment of the *ex-vivo* animal intestine. A segment (500 mm) of fresh porcine colon was attached alongside the fixtures. Then, the colon was arranged to simulate typical anatomical characteristics, such as the angles and alignment of the sigmoid curve and the sharpness of the left colonic flexure.

The capsular device, embedding all the functions described in the previous sections and represented in Fig. 12, was 40 mm in length, 18 mm in diameter and 16.28 g in weight.

Although this capsule is not compatible with swallowing, it allows conservative tests of the magnetic link strength, since both its weight and volume are far more higher than the swallowable capsular device to be used with the presented platform.

The experimental procedure consisted in the following steps:

- (i) The capsule is introduced in the colon specimen.



Fig. 14. Experimental procedure with slightly insufflated colon.

- (ii) The robotic arm is positioned above the phantom and the localization procedure is performed.
- (iii) The EPM is aligned to the IPM streamlines.
- (iv) Once a reliable magnetic link is established, the capsular device is driven by the user along the colon with the aid of the robotic arm, while sending a real time video streaming and information regarding pitch and roll angles to the HMI.

The locomotion pathway was in the antegrade direction, since the final goal of this work is to introduce the wireless device orally.

From experimental tests we achieved, as spatial resolution of the localization process, an average value of 3 cm from the centre of the capsule.

The static magnetic field produced by the EPM and IPM does not cause interference with the electronics inside the capsule. Wireless data transmission was also not affected by the static magnetic field.

The magnetic locomotion was assessed with the colon first insufflated, then collapsed.

In the first case, the localization and orientation control strategy allowed to obtain excellent results and the capsular device managed successfully all the path through the LGI phantom model (Fig. 14). This demonstrates also the proper dimensioning of the magnetic link, since the EPM–IPM interaction was enough to reliably locomote and steer the capsular device throughout the colon.

The robotic platform was tested by several medical doctors that were novel to the procedure. A total number of 40 trials were performed, showing a 100% of success rate in traversing the entire colon. In order to avoid a bias due to direct vision of the capsule inside the LGI simulator, the user was asked to perform the procedure by just looking at the HMI, where real-time image stream from the capsule and the virtual control panel of Fig. 3 are available.

Medical doctors trying the procedure got familiar with the platform and were able to drive the end-effector in an effective way with a short learning curve. The average total time required to travel the entire simulator was almost 10 min, with 7 and 23 min as best and worst times respectively. All users commented very positively the advantages introduced by the inertial feedback, providing real time information about pitch and roll of the endoscopic capsule.



Fig. 15. Experimental procedure with collapsed porcine colon.

In case of collapsed tissues, the capsular device was able to travel only really short areas of the GI tract and manual assistance was required for managing the more difficult regions (Fig. 15). However, the implemented control strategies allowed to effectively execute both the localization and field alignment tasks.

4. Conclusions

The developed robotic platform represents a step forwards in the field of diagnostic and surgical endoluminal procedures, taking advantage of active magnetic locomotion in the GI tract driven by an anthropomorphic robotic arm. Strong potentials for clinical application of this peculiar approach are confirmed already by the Stereotaxis platform¹⁹ and by the significant efforts devoted by Given Imaging Ltd. towards magnetic locomotion.¹⁴

The platform presented in this paper is composed by a HMI and a 6 DOF robotic arm able to move a permanent magnet, interacting with a capsular device by magnetic link. A very high precision of movement can be achieved thanks to the robotic approach, thus enabling a reliable and fine positioning of the endoluminal device.

A novel control strategy based on inertial sensing was conceived to localize the wireless device inside the GI tract and to properly align the EPM to the IPM, thus maximizing magnetic interaction. This solution also allowed a continuous pitch and roll monitoring of the capsular system, thus enabling a useful feedback to the user. This subsystem, including the inertial sensor and a wireless microcontroller, was implemented on a miniaturized circular board (9.6 mm in diameter and 3 mm in thickness), ready to be integrated in a swallowable capsular device.

The robotic platform was extensively tested *ex-vivo*, showing excellent performances for locomotion and steering of a capsular unit inside a slightly insufflated lumen. In the case of collapsed tissue, the capsular device was able to travel only short paths of the GI tract and manual assistance was required to overcome the more collapsed regions. A possible solution to improve system performances in these conditions would be an internal DOF to be placed on board the capsule. This may work in synergy with the external magnetic field, by activating a mechanism inside the capsule, such as legs or vibration, whenever it is required. *In vivo* tests are the next step in order to further support this approach.

A possible improvement in terms of controllability may be obtained by using a double symmetrical EPM system, as in the Stereotaxis platform.¹⁹ This solution is actually under investigation by the authors.

Acknowledgements

The work described in this paper was funded in part by the Intelligent Microsystem Center, KIST, South Korea, and in part by the European Commission in the framework of VECTOR FP6 European project EU/IST-2006-033970. The authors would like to thank novineon Healthcare Technology Partners GmbH, in Tubingen (Germany), for assistance during the testing phase of the device, and Innovent GmbH, Jena (Germany), for the precious discussion towards EPM selection. The tri-axial accelerometer was kindly provided by STMicroelectronics. A special mention to Mr. N. Funaro and E. Susilo for their continuous and invaluable help.

References

1. K. M. Reavis and W. S. Melvin, "Advanced endoscopic technologies," *Surg. Endosc.* **22**, 1533–1546 (2008).
2. M. F. McGee, M. J. Rosen, J. Marks, R. P. Onders, A. Chak, A. Faulx, V. K. Chen and J. Ponsky, "A primer on natural orifice transluminal endoscopic surgery: Building a new paradigm," *Surg. Innovation* **13**, 86–93 (2006).
3. G. J. Iddan and C. P. Swain, "History and development of capsule endoscopy," *Gastrointest. Endosc.* **14**, 1–9 (2004).
4. G. Iddan, G. Meron, A. Glukhoysky and P. Swain, "Wireless capsule endoscopy," *Nature* **405**, 405–417 (2000).
5. A. Moglia, A. Menciassi, M. O. Schurr and P. Dario, "Wireless capsule endoscopy: From diagnostic devices to multipurpose robotic systems," *Biomed. Microdevices* **9**, 235–243 (2007).
6. A. Moglia, A. Menciassia, P. Dario and A. Cuschieri, "Clinical update: Endoscopy for small-bowel tumors", *The Lancet* **370**, 114–116 (2007).
7. VECTOR European Project website. Available on: <http://www.vector-project.com>. Last accessed August 2009.
8. A. Menciassi, M. Quirini and P. Dario, "Microrobotics for future gastrointestinal endoscopy," *Minim. Invasive Therapy Allied Technol.* **16**, 91–100 (2007).
9. H. Park, S. Park, E. Yoon, B. Kim, J. Park and S. Park, "Paddling Based Microrobot for Capsule Endoscopes," *Proceedings of IEEE International Conference on Robotics and Automation*, Rome, Italy (Apr. 2007) pp. 3377–3382.
10. M. Quirini, S. Scapellato, A. Menciassi, P. Dario, F. Rieber, C. N. Ho, S. Schostek and M. O. Schurr, "Feasibility proof of a legged locomotion capsule for the GI tract," *Gastrointest. Endosc.* **67**, 1153–1158 (2008).
11. M. Quirini, R. Webster, A. Menciassi and P. Dario, "Design of a Pillsized 12-Legged Endoscopic Capsule Robot," *Proceedings of IEEE International Conference on Robotics and Automation*, Rome, Italy (Apr. 2007) pp. 1856–1862.
12. R. Sidhu, D. S. Sanders and M. E. McAlindon, "Gastrointestinal capsule endoscopy: From tertiary centres to primary care," *Br. Med. J.* **332**, 528–531 (2006).
13. F. Carpi, S. Galbiati and A. Carpi, "Controlled navigation of endoscopic capsules: Concept and preliminary experimental investigations," *IEEE Trans. Biomed. Eng.* **54**, 2028–2036 (2007).
14. F. Volke, J. Keller, A. Schneider, J. Gerber, M. Reimann-Zawadzki, E. Rabinovitz, C. A. Mosse and P. Swain, "In-vivo remote manipulation of modified capsule endoscopes using an external magnetic field," *Gastrointest. Endosc.* **5**, AB121–AB122 (2008).
15. Olympus Endocapsule. Available on: <http://www.olympus-europa.com/endoscopy/>. Last accessed August 2009.
16. X. Wang and M. Q. H. Meng, "A Magnetic Stereo Actuation Mechanism for Active Capsule Endoscope," *Proceedings of IEEE International Conference on Engineering in Medicine and Biology Society*, Lyon, France (Sep. 2007) pp. 2811–2814.
17. J. J. Abbott, O. Ergeneman, M. P. Kummer, A. M. Hirt and B. J. Nelson, "Modeling magnetic torque and force for controlled manipulation of soft-magnetic bodies," *IEEE Trans. Robot.* **23**, 1247–1252 (2007).
18. S. Tamaz, R. Gourdeau, A. Chanu, J. B. Mathieu and S. Martel, "Real-time MRI-based control of a ferromagnetic core for endovascular navigation," *IEEE Trans. Biomed. Eng.* **55**, 1854–1863 (2008).
19. Stereotaxis website. Available on: <http://www.stereotaxis.com>. Last accessed August 2009.
20. J. S. Agashe and D. P. Arnold, "A study of scaling and geometry effects on the forces between cuboidal and cylindrical magnets using analytical force solution," *J. Phys. D: Appl. Phys.* **41**, 105001-1-9 (2008).
21. B. Manz, M. Benecke and F. Volke, "A simple, small and low cost permanent magnet design to produce homogeneous magnetic fields," *J. Magn. Reson.* **192**, 131–138 (2008).
22. R. Glaser, *Biophysics* (Springer, Heidelberg, Germany, 2001).
23. NDI The Aurora Electromagnetic Measurement System. Available on: <http://www.ndigital.com>. Last accessed August 2009.